This is a preprint version of the article: Štěpán, P., Kulich, M., and Přeučil, L. (2005). **Robust Data Fusion with Occupancy Grid**. *IEEE Transactions on Systems, Man, and Cybernetics: Part C*, 35(1), which has been published in a final form at https://doi.org/10.1109/TSMCC.2004.840048.

Robust Data Fusion with Occupancy Grid

Petr Štěpán, Miroslav Kulich, and Libor Přeučil

***Abstract*— Accurate models of the environment are a crucial requirement for autonomous mobile robots. The process of how to acquire knowledge about the operating environment is one of the most challenging problems in this research area. The quality of the model depends on the number and types of sensors used. Occupancy grids are the most common low-level models of the environment used in robotics for fusion of noisy data. This paper first introduces a novel method for building an occupancy grid from a monocular color camera. The next part of the work describes a method for fusion of camera data with data from a rangefinder. The final part presents a new method for measuring the quality of the occupancy grid based on the quality of the path created by the grid. The methods were experimentally verified with an indoor experimental robot at the Czech Technical University.**

***Index Terms*— data fusion, camera, laser rangefinder, sonar, occupancy grids.**

I. Introduction

STANDARD data fusion methods used for navigation tasks in mobile robotics incorporate integration of data from sets of on-board sensors of the same type, or at least of those based on similar sensing principles. Typical classes for such sensors are range finders, data from other localization systems, etc. As the goal is to achieve maximum robustness of after-fusion data, it is assumed that further improvements might be obtained by direct integration across different kind of sensing systems. It is expected, that this will introduce new possibilities in the fusion field. The expectation is to bring better performance through exploring capabilities to combine multiple sources in situations when some sensors fail. A straightforward candidate for this is direct fusion of range measuring devices with intensity images using the occupancy grid approach.

The first step in building the occupancy grid is to solve the localization task. It is supposed that localization is achieved by landmark-based localization or Markov localization. The main idea of landmark localization is to detect and match characteristic features in the environment [1]. The Markov localization evaluates a probability distribution over the space of possible robot states that represent position [2]. Robust sensor matching techniques compare raw or pre-processed sets of data obtained from range sensors with a map or previously gathered measurement. A promising extension to line-to-line matching has been applied in [3].

Having solved the localization task, other sensors can be integrated to improve robot navigation in the partially known environment. Major attention is devoted to integrating monocular color camera into the navigation process and building the world model. The task setup is constrained to situations in which the robot operates on flat surfaces. The typical situation appears in indoor environments or even outdoors, where this condition is partially satisfied on roads [4].

The fusion is based on the occupancy grid introduced in [5]. Building an occupancy grid from monocular camera data is the central part of the method introduced in this paper. Knowing the position of some obstacles from range measurements can improve and calibrate the probability profiles for the camera sensor. The combination of diverse sensors like range finders and monocular camera in the approach leads to more accurate 2D maps of the environment. The accuracy of the grid is evaluated using a path-planning algorithm. The objective function for path quality is the accuracy of the environmental model.

II. Occupancy grid from monocular camera

Occupancy grids are the most common low-level sensor-based models of the environment used in robotics. The occupancy grid approach is very robust for fusion of noisy data but its application field has previously been limited to exclusive use with range sensors (it was originally designed for sonar data fusion). The following shows that under certain but reasonable circumstances the occupancy grid concept can also be used for fusion of monocular camera data.

A central assumption guaranteeing admissibility of the method is that the robot operates on a flat ground-plane. This assumption enables us to determine all parameters of the robot system. This approach can be used even if this condition is satisfied partially, for example on roads (see [4]). In this case, the parameters of the camera system can be calibrated and afterwards used to detect obstacles in the robot's surroundings.

A. Inverse perspective transformation

The goal is to obtain a 2D map of the robot's-operating environment. It is necessary to find parameters of the robot system to evaluate the transformation from the image coordinate system (u, v) into the robot coordinate system (x, y) - see figure 1. This means to determine the projection function $f(u, v) = (x, y)$.

The first step is a reduction of the radial distortion and decentering [6]. The constants u_c, v_c and p_1, p_2, p_3 can be determined from a calibration pattern according to the following equations:

$$dist(u,v) = (u-u_c)^2 + (v-v_c)^2 \quad (1)$$

$$u'(u,v) = (u-u_c)(1 + p_1 dist(u,v) + p_2 dist(u,v)^2 + p_3 dist(u,v)^3) \quad (2)$$

$$v'(u,v) = (v-v_c)(1 + p_1 dist(u,v) + p_2 dist(u,v)^2 + p_3 dist(u,v)^3) \quad (3)$$

P. Štěpán and L. Přeučil are with Department of Cybernetics, Czech Technical University.

M. Kulich is with Center of Applied Cybernetics, Czech Technical University.

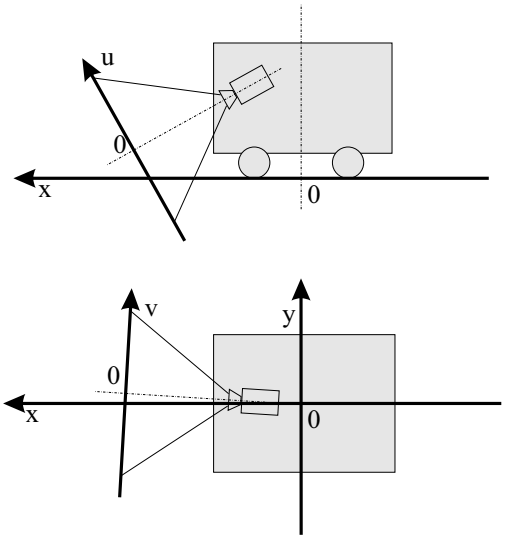

Fig. 1. Coordinate systems for the mobile robot onboard camera

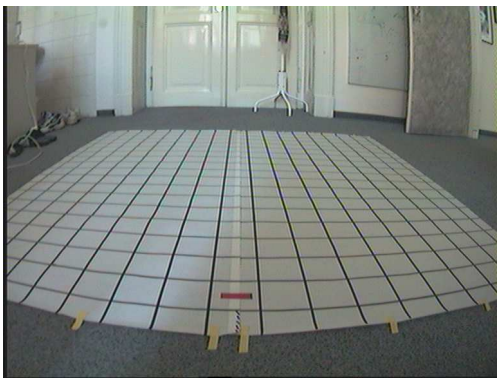

Fig. 2. Calibration pattern for radial distortion

To set the parameters of radial distortion and decentering, the pattern from the figure 2 was used. The image is used to detect points on lines and then minimize the square distance of these points to corresponding lines. The result of this minimization are the u_c, v_c and p_1, p_2, p_3 parameters. The pair (u', v') determines the coordinates of the image after correction of the radial distortion. The result of this step is depicted in figure 3.

The next step is to detect the shift of the camera from the center of the robot x_{cam}, y_{cam}, and parameters of the plane that describes the floor of the environment, Δu, Δv, X and Y. The following equations describe the inverse projective transformation:

$$x_0(u', v') = -\frac{(u' - \Delta u)X}{v' - \Delta v} + x_{cam} \quad (4)$$

$$y_0(u', v') = -\frac{Y}{v' - \Delta v} + y_{cam}, \quad (5)$$

Fig. 3. Image after removing the radial distortion

A complete transformation is required to correct the angular deviation of the camera axis and the robot axis α as well as to obtain the coordinates in the robot world. Assuming, the robot position is x_{rob}, y_{rob}, ω_{rob}, the complete transformation to the world coordinate system can be described as:

$$\begin{aligned} x(x_0, y_0) &= x_{rob} + x_0 \cos(\alpha + \omega_{rob}) \\ &\quad - y_0 \sin(\alpha + \omega_{rob}) \quad (6) \\ y(x_0, y_0) &= y_{rob} + x_0 \sin(\alpha + \omega_{rob}) \\ &\quad + y_0 \cos(\alpha + \omega_{rob}) \quad (7) \end{aligned}$$

Eleven measurements of a reference box were done by camera and laser range finder to determine all the parameters Δu, Δv, X, Y, x_{cam}, y_{cam}, α mentioned above. Each camera measurement represents four points (the borders of the box and two points on the front side) and the laser range finder provides the real position of this box. Minimization of the square distance between the real and the computed position in the camera image produces parameters x_{cam}, y_{cam}, Δu, Δv, X, Y, α of the robot's camera system.

B. Definition of the Probability Profiles

The first approach to detection of free space is done making use of the color of the floor. Suppose that the color is different from the obstacle surface color. If the color of the floor is known the probability distribution of free space can be defined.

The occupancy grid [5] is built using the Bayes' update formula:

$$P^{Occ}(c|R) = \frac{p^{Occ}(R|c)P^{Occ}(c)}{p^{Occ}(R|c)P^{Occ}(c) + p^{Emp}(R|c)P^{Emp}(c)} \quad (8)$$

where:

$$P^{Emp}(c) = 1 - P^{Occ}(c) \quad (9)$$

$$p^{Emp}(R|c) = 1 - p^{Occ}(R|c) \quad (10)$$

The equation (8) defines the conditional probability $P^{Occ}(c|R)$, that the cell c is occupied given the measured color reading $R = (h, s, v)$. The probability depends on the old value of the cell from the grid $P^{Occ}(c)$ and the probability distribution $p^{Occ}(R|c)$. The probability distribution $p^{Occ}(R|c)$ can be represented as the difference of the measured color R and the reference color of the floor in the hsv-space. The

following can be used to compute the conditional probability depending on the reference color of the floor (h_r, s_r, v_r):

$$dif(x) = e^{-\frac{x^2}{2\sigma^2}} \quad (11)$$

$$p^{Occ}(R|c) = dif(h-h_r)dif(s-s_r) \; dif(v-v_r), \quad (12)$$

where σ represents the sensitivity of the difference function.

C. Calibration of the Probability Profiles with Range-Data

If the color of the floor is similar to the color of the obstacles, the previous method fails. The following approach uses definition of profiles $p^{Occ}(R|c)$ supported by additional information about the environment.

The additional information can be either a map of a training environment or combination of sonar and laser data, which can accurately measure the training environment. The probability profiles can then be calculated directly from the camera images. The free space and the border of the obstacle is determined from the range finder data or from the training map of the environment.

The probability distribution is defined by matrices f for free colors and o for occupancy colors. The matrices f and o represent hsv-color space and denote the number of cells of a specific color that are free, and respectively occupied. In our example, 10 images captured under different lighting conditions were used to create the matrixes f and o with dimension $20 \times 20 \times 20$. For each pixel of the camera image, the occupancy of this pixel in the robot's coordinate system was calculated for range measurement. If the pixel with color $(h, s, v) \in < 0, 1 >^3$ represents a free space then the matrix value $f(\lceil 20h \rceil, \lceil 20s \rceil, \lceil 20v \rceil)$ is increased. If the pixel belongs to the occupied space, the matrix value $o(\lceil 20h \rceil, \lceil 20s \rceil, \lceil 20v \rceil)$ is increased. The probability profile $p^{Occ}(R|c)$ for reading $R = (h, s, v)$ is defined by the following formula:

$$p^{Occ}(R|c) = \begin{cases} \frac{o(h',s',v')}{f(h',s',v')+o(h',s',v')} & \text{if } f(h',s',v')+ \\ & o(h',s',v') > 0 \\ 1 & \text{otherwise} \end{cases} \quad (13)$$

The parameters h', s', and v' stand for $h' = \lceil 20h \rceil$, $s' = \lceil 20s \rceil$, $v' = \lceil 20v \rceil$. Figure 4 shows the original image from the onboard camera, while figure 5 shows the same image after transformation to the robot's coordination system, where each pixel defines a 5×5 cm cell of the robot environment. Finally figure 6 depicts the occupancy grid created using probability profile matrices of dimension $20 \times 20 \times 20$

The robot position is located at the bottom side of the picture and the camera is oriented upwards in this case. White color indicates free space as detected by the color probability profile of the floor plane.

D. Occupancy Grid Postprocessing

The final occupancy grid construction incorporates information about visibility. When the camera detects any obstacle, free space behind the obstacle is not visible and therefore considered as occupied. Optionally the color of the floor can appear on the obstacle and then produces wrong detection,

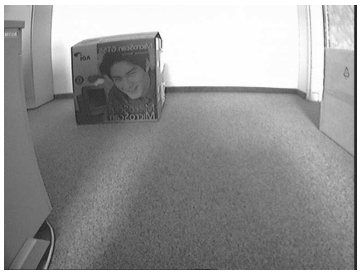

Fig. 4. The original onboard camera image

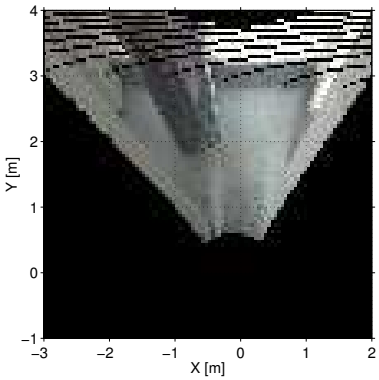

Fig. 5. The image transformed into robot coordinates

even when the border of the obstacle is detected very well. Therefore, only those grid cells are adapted that lie in the region from the position of the robot to the border of the first detected obstacle.

Adaptation of the occupancy grid is performed sequentially from the camera position to the border of the camera visual field. For each grid cell c, an accumulated probability of free space is defined by composition of probabilities of all cells preceding c in the camera view. Let C denote the set of cells on a beam from the robot position to the position of cell c. The accumulated probability is computed applying the following formula:

$$P^{Occ}_{new}(c) = P^{Occ}(c)P^{Occ}_{Acc}(C) \quad (14)$$

There are two basic possibilities for how the accumulated probability $P^{Occ}_{Acc}(C)$ can be defined. The first one is a simple product of the probabilities of all cells from the viewpoint. The second approach uses the Bayes' formula for recursive definition of this probability:

$$P^{Occ}_{Acc}(C \cup \{c\}) = \frac{P^{Occ}(c)P^{Occ}_{Acc}(C)}{P^{Occ}(c)P^{Occ}_{Acc}(C)+(1-P^{Occ}(c))(1-P^{Occ}_{Acc}(C))} \quad (15)$$

The next step, which improves robustness of map building, is detection of a border of the nearest obstacle in the particular direction. In our case a simple threshold is used, which eliminates local occlusions in the direction from the robot to the detected obstacle [6]. An obstacle is detected if the accumulated probability is less than a defined threshold for three succeeding grid cells. Moreover, a filtration process to remove measurement outliers can follow the thresholding process.

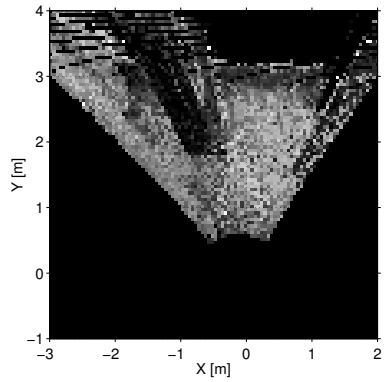

Fig. 6. The occupancy grid (left) and the occupancy grid after postprocessing (right)

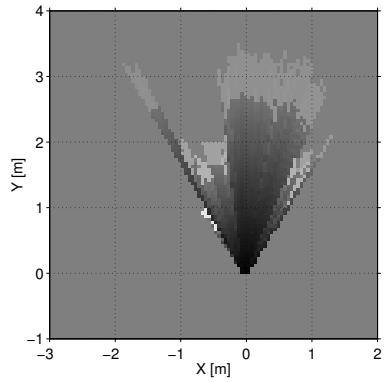

Fig. 7. The occupancy grid (left) and the occupancy grid after postprocessing (right)

The approach described above results in smoothed range measurements of the scene visible from the camera. The filtered data are very similar to rangefinder data and these measurements are used to build an occupancy grid in a similar way to rangefinder data [7]. To build the occupancy grid a model of sensor accuracy with respect to measured distance has to be defined.

The angle accuracy of the camera system was experimentally set to ± 2 pixels. This accuracy depends on the smoothness of the floor and on admissible vibration of the robot during movement.

Considering equation (5) the accuracy of the sensor in depth can be expressed as $y(u',v') - y(u',v'+2)$. For pixel (u',v') this formula can be transformed to the following equation:

$$y(u',v') - y(u',v'+2) = \frac{Y}{v'^2 + v'(1 - 2 * \Delta v) + \Delta v^2} \quad (16)$$

Suppose the accuracy of the sensor is defined by function $\xi(d)$ that is represented by equation $\xi(y(u,v)) = y(u,v) - y(u,v+2)$. The shape of the function $\xi(d)$ is depicted in fig. 8. The function $\xi(d)$ can be approximated by a quadratic function.

The final model of camera sensor based on measured

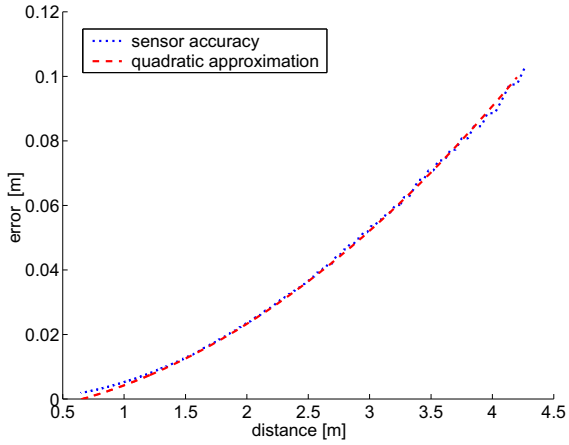

Fig. 8. Accuracy of the camera system with respect to detected distance.

distance is following (similar to sonar sensor, see [7]):

$$p^{Occ}(R|c) = \begin{cases} \frac{d}{2\cdot(r-\xi(r))} & \text{if } d \in < 0, r - \xi(r) > \\ \frac{1+\xi(r)}{2\cdot\xi(r)} & \text{if } d \in (r - \xi(r), r + \xi(r) > \\ 0 & \text{otherwise} \end{cases} \quad (17)$$

where r is the detected distance in measurement R and d is the distance of cell c from the robot position. Additional information about visibility is used to improve the final result from the color camera, with reduced image noise and taking into account the accuracy of the camera sensor. Figure 7 shows the result of application camera model to image from figure 6.

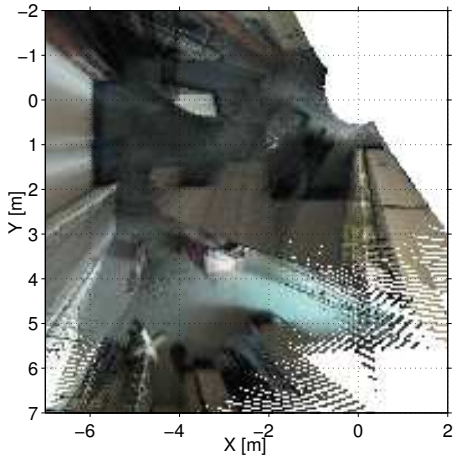

Fig. 9. Superimposion of he original camera data in typical office environment

The superimposed data from color camera is depicted in figure 9. Figure 10 shows the final occupancy grid. This experiment was done in a typical office environment without additional changes.

III. Combination of data from sonar and camera

In this section three approaches for fusion of data from sonar rangefinder, laser rangefinder and monocular camera using occupancy grids are introduced. The first method is based on

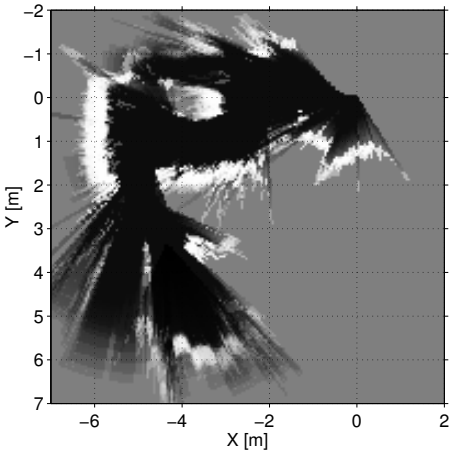

Fig. 10. Final occupancy grid using data from figure 9

simple fusion in one occupancy grid. Due to incompatibility of different types of sensors, some cases cannot be solved using a single occupancy grid. Therefore the second approach is suggested. This approach uses two separate grids and the final grid is the fusion of these two grids.

A. Fusion of sensors with one occupancy grid

The simplest method is integration of different sensors into one grid. Both sensors share the same grid for global information about environment. Data from different sensors can vary in frequency and quality of measurements and hence measures of sensor models are not comparable. The variability of sensor models does not allow fusing data directly to one common grid whenever gathered by sensors. This disadvantage can be reduced by filtration of false measurements. Filtration of sonar measurement using data from laser rangefinder is proposed in [8].

B. Fusion of sensors with two occupancy grids

In this method an occupancy grid is constructed for each sensor type and these grids are used to build a resulting grid. If the accuracy of a sensor is not taken into account, a value of a cell in the resulting grid can be computed by combining the corresponding cells in the source grids. This fusion differs from the standard fusion during construction of the grid, as it is necessary to determine occupancy of the cell if at least one sensor detects the obstacle.

Two rules are applied to obtain the resulting probability:

- If at least one of the source cells has higher probability that it represents occupied space than a predefined threshold T_{Occ}, the probability of the resulting cell is set to 1.
- Bayes' rule is applied otherwise.

More precisely, the resulting grid is computed in two steps. Values in the source grids are modified first using the following formula:

$$P^{Occ}_{mod}(c) = \begin{cases} 1 & \text{for } P^{Occ}(c) > T_{Occ}, \\ \frac{P^{Occ}(c)+T_{Occ}-1}{2\cdot T_{Occ}-1} & \text{for } P^{Occ}(c) \in <0.5, T_{Occ}> \\ P^{Occ}(c) & \text{otherwise} \end{cases} \tag{18}$$

The computed values are than applied in Bayes' rule to obtain probabilities in the resulting grid:

$$P^{Occ}_{fuse}(c) = \frac{P^{Occ}_1(c)P^{Occ}_2(c)}{P^{Occ}_1(c)P^{Occ}_2(c) + (1-P^{Occ}_1(c)(1-P^{Occ}_2(c))} \tag{19}$$

where P^{Occ}_1 is the modified probability of occupancy from the first sensor, $P^{Occ}_{sensor2}$ is the modified probability of occupancy from the second sensor, and the P^{Occ}_{fuse} is probability of occupancy after data fusion.

C. Fusion of sensors with different precision

The grid built from sonar measurements has a precision depending on the precision of the sonar but also the distortion imposed by the shape of the sonar signal has to be taken into account. This means that one point in the environment can impact several neighboring cells. Therefore, when fusing data from sonar and a more precise sensor like a camera, it is useful to combine a value from one cell in the camera grid with a small neighborhood of the corresponding cell in the sonar grid. If an occupied space is detected by the camera in any cell but not detected in the corresponding neighborhood by sonar, then the sonar measurements are canceled. The cell value in the resulting grid is equal to the value in the camera grid.

Suppose that the parameter acc defines the additional inaccuracy of the sonar sensor. Then we can define the probability of occupancy cell with coordination (x, y) as follows:

$$P^{Occ}_{neigh}(cell_{(x,y)}) = \max_{\substack{x-acc\le i\le x+acc,\\ y-acc\le j\le y+acc}} P^{Occ}(cell_{(i,j)}) \tag{20}$$

The sensor fusion is done with respect to probability of occupancy from the neighborhood of the less accurate sensor, in our case, from the sonar sensor. The final probability is defined by:

$$P^{Occ}_{fuse}(c) = \begin{cases} \frac{P^{Occ}_1(c)P^{Occ}_2(c)}{P^{Occ}_1(l)P^{Occ}_2(c)+(1-P^{Occ}_1(c))(1-P^{Occ}_2(c))}, \\ \quad \text{if } P^{Occ}_{neigh}(c) > T_{Occ} \\ P^{Occ}_2(c), \quad \text{otherwise} \end{cases} \tag{21}$$

IV. Planning with occupancy grid

The above mentioned occupancy grid can be used for path planning with a harmonic potential field. The core property of the harmonic potential field is having only a single local minimum and therefore the planning algorithm cannot fail [9]. The harmonic potential field $U(q)$ is defined on the set Ω as a function that satisfies Laplace's equation:

$$\nabla^2 U(q) = 0 \tag{22}$$

For planning purposes the borders of the set Ω are defined as borders of the obstacles and the desired final robot position. The harmonic potential field has to satisfy these border conditions:

$$U|_{\partial\Omega} = 0 \tag{23}$$

$$U(goal) = const \tag{24}$$

The proof that the potential field has no other local minimum than the global one is in [10]. The harmonic potential field can be computed by numeric approximation of Laplace's equation [11]. Using a grid with constant cell size, the second derivation can be enumerated by Taylor's formula and a system of linear equations is reached. This system can be solved by Gauss-Seidel's iteration. The k^{th}-step of Gauss-Seidel's iteration can be computed by the following equation:

$$\begin{aligned} U^{k+1}(x_i, y_j) &= \frac{1}{4} \cdot (U^k(x_{i+1}, y_j) + U^{k+1}(x_{i-1}, y_j) \\ &\quad + U^k(x_i, y_{j+1}) \\ &\quad + U^{k+1}(x_i, y_{j-1})) \end{aligned} \tag{25}$$

The number of iterations depends on the length of the final path. The size of the grid can estimate the maximal length of reasonable paths and this limit serves as the number of iteration steps. The path from position (i, j) to the goal position exists if and only if the value $U(i, j) > 0$. The path can be found as an increasing sequence for (i, j) to the goal position. The successor of the cell is the cell from eight-neighborhood with maximal value of potential field.

A. Preprocessing of grid for planning

The goal position and borders of the obstacles define the potential field. The path is found for the robot with zero size. In our case the size of the robot is approximated by a circle and the obstacles in the grid have to be enlarged by the diameter of the robot. In addition the grid is changed to find the optimal safe trajectory.

The obstacles are segmented from the grid and the morphological operation erosion enlarges the obstacles by the diameter of the robot. The second step changes the grid in order to find path that is planned in some safe distance from the obstacles. It is necessary to keep the property that the path can be found even if the corridor is narrow. The second step is represented by following equation:

$$M^{k+1}(i, j) = \max(M^k(i, j), \max_{\substack{i-1 \le a \le i+1, \\ j-1 \le b \le j+1}} M^k(a, b) - step), \tag{26}$$

where $step = \frac{cell_{size}}{safe_{distance}}$ is the coefficient for decreasing the grid occupancy depending on the cell size and safe distance.

The final changed occupancy grid $M'$is used for iterative computation of the harmonic potential field using the following equation:

$$\begin{aligned} U^{k+1}(x_i, y_j) &= \frac{1 - M'(x_i, y_j)}{4} \cdot (U^k(x_{i+1}, y_j) \\ &\quad + U^{k+1}(x_{i-1}, y_j) \\ &\quad + U^k(x_i, y_{j+1}) + U^{k+1}(x_i, y_{j-1})) \end{aligned} \tag{27}$$

The occupancy grid, changed occupancy grid and the final harmonic potential field with planned path is depicted in figure 11.

V. Evaluation of the fusion methods

Different measures can be defined to evaluate the quality of the occupancy grid. In [12], the measure is defined as the correlation of the computed grid with a pattern grid. This method does not describe the quality of the grid with respect to using the grid for planning. This is why a new safety measure is introduced. Other methods do not evaluate the quality of the grid with respect to the path planning process. The advantage of our approach is that this measure can help to select the best fusion method and best sensor types for a specific environment. It can also be used to calculate the reliability of planning and data fusion algorithms.

TABLE I

Safety of path depending on the fusion methods and sensors

method and sensors	safety of the path ($safety$ / $\overline{safety}$) [cell] data from figure 12		
	normal env.	doorways	low obstacles
sonar	7 / 9.1290	0 / 9.1429	5 / 6.7500
laser	8 / 9.2903	7 / 9.2857	2 / 5.2500
camera	6 / 8.7419	7 / 8.4286	6 / 6.6250
sonar+laser one grid	8 / 9.3871	7 / 9.3571	2 / 5.1250
sonar+laser one grid and filtration	8 / 9.3871	7 / 9.3571	4 / 6.8750
sonar+laser two grids	8 / 9.3548	0 / 9.2143	6 / 7.2500
sonar+laser two grids different accuracy	8 / 9.2903	0 / 9.0000	6 / 7.2500
sonar+laser two grid and filtration	0 / 9.0968	6 / 9.2857	6 / 7.2500
sonar+laser two grids and filtration different accuracy	6 / 9.0645	6 / 9.2143	6 / 7.2500
camera + sonar one grid	8 / 8 / 9.2258	7 / 7 / 9.0000	7 / 7.3750
camera + sonar two grids	0 / 9.0645	0 / 9.0714	6 / 7.1250
camera + sonar two grids different accuracy	6 / 9.0000	0 / 8.9286	6 / 7.0000

The safety measure can be computed from the planned path and pattern grid. Let P_M be a path defined by grid M from actual robot position to a goal that is inside of this grid. The path $P_M = \{p_i\}_{i=0}^{n}$ is defined as a sequence of n cells p_i. The pattern grid defines function $dist(p_i)$, that represents the minimal distance from cell p_i to the obstacle.

The safety of the grid M is defined by the safety of the path P_M that was planned using grid M. The safety of the path P_M is defined as follows:

$$safety(M) = safety(P_M) = \min_{i=0..n} (dist(p_i)) \tag{28}$$

If the $safety(M)$ of the grid M is less than the diameter of the robot, the grid cannot be used for planning a path. The bigger the $safety(M)$, the better grid M represents the environment. For grid comparison an average safety can be computed as:

$$\overline{safety}(M) = \overline{safety}(P_M) = \sum_{i=0}^{n} \frac{dist(p_i)}{n} \tag{29}$$

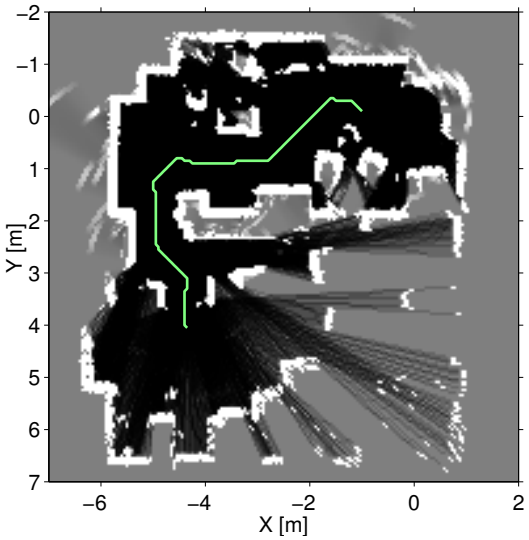

(a) Occupancy grid with planned path

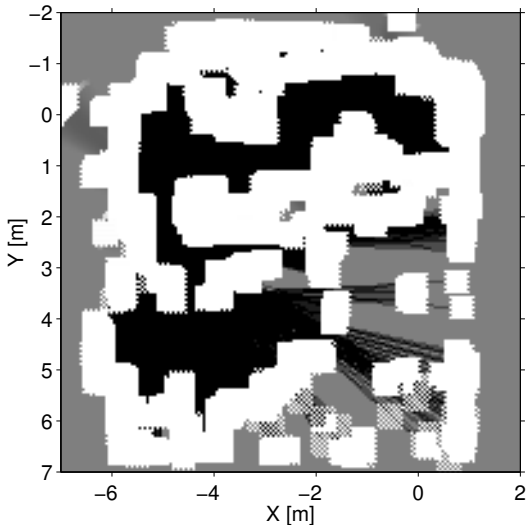

(b) Enlargement of the obstacles

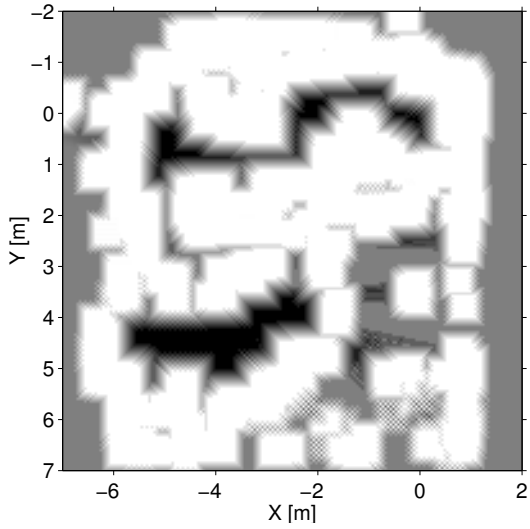

(c) Grid changed for safe path

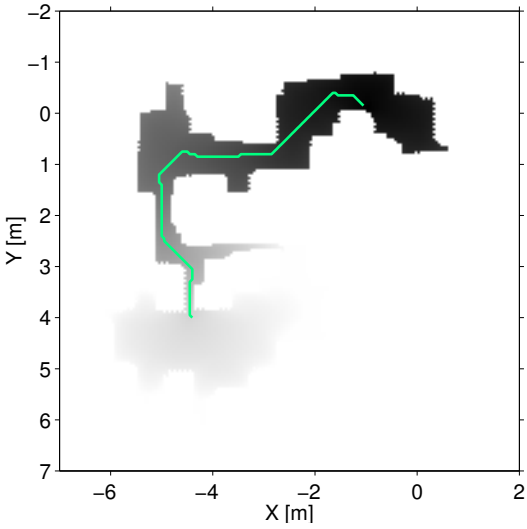

(d) Final potential field with planned path

Fig. 11. Example of planning algorithm with harmonic potential field

A. *Experimental evaluation*

The experiment depicted in fig.12 was performed in a typical office environment. This environment has two examples of problems with sensing. The experiment was done in two rooms connected by a door. Doorways are problematic for sonar sensors as sonar uses a wide beam and often cannot detect the free space inside the door. The second problem was in two boxes that were too low to be visible for the laser rangefinder. These boxes were in the lower room.

The results of the safety measure for different sensors and different fusion methods are listed in table I. The values in the table represent the minimum distance to the obstacle in cell units. This means that for cell size $10cm \times 10cm$ the value multiplied by $10cm$ is the distance to the nearest obstacle for the whole path. The experiment was divided to three parts to show the sensitivity of the fusion methods in different types of environment. The normal environment represents a typical office environment. The doorway data set contains data of the robot moving through the door. The low obstacles data set represents data when the robot passes around obstacles that are to low to be detected by laser rangefinder.

The figure 13 depicts some examples of planned paths through doorway and around the lower boxes. You can notice that laser-ranging fails for the environment with boxes (see figure 13(d)), because the diameter of the robot was $4\ cells$ and the safety of some path was $2\ cells$. These boxes were detected only by the sonar and camera. Navigation done exclusively with laser rangefinder will lead to collision. The sonar fails

for the doorway and finds a nonsense path (see figure 13(b)).

The experiments have shown that the most efficient method for fusion of sonar and laser data is fusion with two grids incorporating the accuracy of sensors. As the camera and the sonar have more or less similar properties, the best method for fusion is using one occupancy grid or two grids with different sensor accuracies.

VI. Conclusion

The problem of environment modeling for autonomous mobile robots is a challenging field with many open problems. The environment model recovery strongly depends on the localization problem. As there still does not exist any unified approach to reliable recovery of environment models, the robustness is typically improved through data and model fusion from multiple sources.

It has been illustrated, that under assumption that the robot operates in environment with more or less uniform and flat ground-plane (floors, road, etc.) the occupancy grid can be extended towards data fusion from monocular camera. This improves the robustness and accuracy while building environment models in mobile robotics.

The early achievements of the described approach were experimentally verified with real data in real indoor environments. Respecting the limited space of this contribution, selected results were briefly illustrated in the text above.

Acknowledgment

The work was supported by the European Community under the IST programme "Future and Emerging Technologies" within the project IST-2001-38873, the Ministry of Education of the Czech Republic within the frame of the project "Decision-Making and Control for Manufacturing" number MSM 212300013. The support of the Ministry of Education of the Czech Republic, under the Project No. LN00B096 to Miroslav Kulich, is also gratefully acknowledged.

References

[1] J. Leonard, I. Cox, and H. F. Durrant-Whyte, "Dynamic map building for an autonomous mobile robot," in *Proceedings of the IEEE International Workshop on Intelligent Robots and Systems*. Stuttgart,Germany, 1990, pp. 89–96.

[2] D. Fox, W. Burgard, and S. Thrun, "Markov localization for mobile robots in dynamic environments," *IEEE transactions on systems, man, and cybernetics*, vol. 11, pp. 391–427, 1999.

[3] B. Chmelař, L. Přeučil, and P. Štěpán, "Range-data based position localization and refinement for a mobile robot," in *Proceedings of the 6th IFAC Symposium on Robot Control*. Vienna, Austria, 2000, pp. 364–379.

[4] A. Broggi, M. Bertozzi, and A. Fascioli, "An extension to the inverse perspective mapping to handle non-flat roads," in *Proceedings of the IEEE International Conference on Intelligent Vehicles*. Stuttgart,Germany, 1998, pp. 305–309.

[5] A. Elfes, "Occupancy grids: A probabilistic framework fo robot perception and navigation," Ph.D. dissertation, Electrical and Computer Engineering Department/Robotics Institute, Carnegie-Mellon University, May 1989.

[6] M. Šonka, V. Hlaváč, and R. Boyle, *Image Processing, Analysis and Machine Vision*. Beijing, China: Thomson Asia Pte Ltd., 2002.

[7] P. Štěpán, L. Král, M. Kulich, and L. Přeučil, "Open control architecture for mobile robot," in *Proceedings of the 14th World Congress of IFAC*, vol. Q. Beijing, China: IFAC, July 1999, pp. 163–169.

[8] P. Štěpán, "Internal representation of environment for autonomous mobile robots," Ph.D. dissertation, Dept. of cybernetics, Czech Technical University in Prague, April 2002.

[9] C. Connolly and C. Grupen, "The application of harmonic functions to robotics," *Journal of Robotic Systems*, vol. 10, no. 7, pp. 931–946, 1993.

[10] R. Courant and D. Hilbert, *Methods of Mathematical Physics, I*. New York, NY: Interscience, 1953.

[11] C. Connolly, "Harmonic functions and collision probabilities," in *IEEE International Conference on Robotics and Automation*. IEEE, May 1994, pp. 3015–3019.

[12] M. Martin and H. Moravec, "Robot evidence grid," The robotics Institute, Carnegie Mellon University, Pittsburgh, Pennsylvania, Tech. Rep. CMU-RI-TR-96-06, March 1996.

Petr Štěpán obtained MSc. degree in Theoretical Cybernetics from the Charles University, Prague in 1994 and completed Ph.D. degree in AI at the Czech Technical University in 2002. Since 1996 he has been research fellow at the Gerstner Laboratory for Intelligent Decision Making and Control at CTU. Since 1998 he has been working on verification of software specification and has created simulation software for automation of railway traffic. His interests include data fusion, data analysis, and methods for formal specification and software testing. He is a co-author of about 30 publications in proceedings of international conferences. He was involved within two projects INCO Copernicus and IST FET.

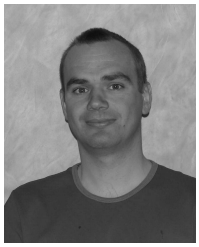

Miroslav Kulich obtained MSc. degree in Software Systems from the Charles University, Prague in 1996 and receiveded Ph.D. degree in localization and mapping for autonomous mobile robots in 2004. His expertise covers data fusion and interpretation, intelligent robotics, and software testing automation. Since 1999, he also participates in testing and development of software for pacemakers and since 2000 has been research fellow in the Center of Applied Cybernetics. He is a co-author of the control system for an autonomous mobile robot. Miroslav Kulich is an author or co-author of about 20 publications in the above-mentioned area.

Libor Přeučil Head of the robotic group at Department of Cybernetics at the CTU Prague. (Ph.D. in computer vision and medical image processing, 1993, FEE-CTU Prague) Since 1996 he has acted as the Managing Researcher at the Gerstner Laboratory, CTU Prague. He is a senior research fellow being involved in or lead many projects within the TEMPUS, INCO Copernicus, Czech Grant Agency, University Development Fund, etc. and multiple industrial contracts. Currently his research interest focuses on the area of intelligent robotics: control of self-guided autonomous vehicles, namely uncertain sensory information processing, and design and development of methodologies for robust software design and testing. He is an author or co-author of about 50 publications in proceedings of international conferences, journal papers and co-author of two textbooks on AI and one edited book published by Springer-Verlag. Besides that he is an active member of the IFAC Workgroup for Autonomous Vehicles and member of a program committee of the Information Technology in Mechatronics (ITM'01) conference.

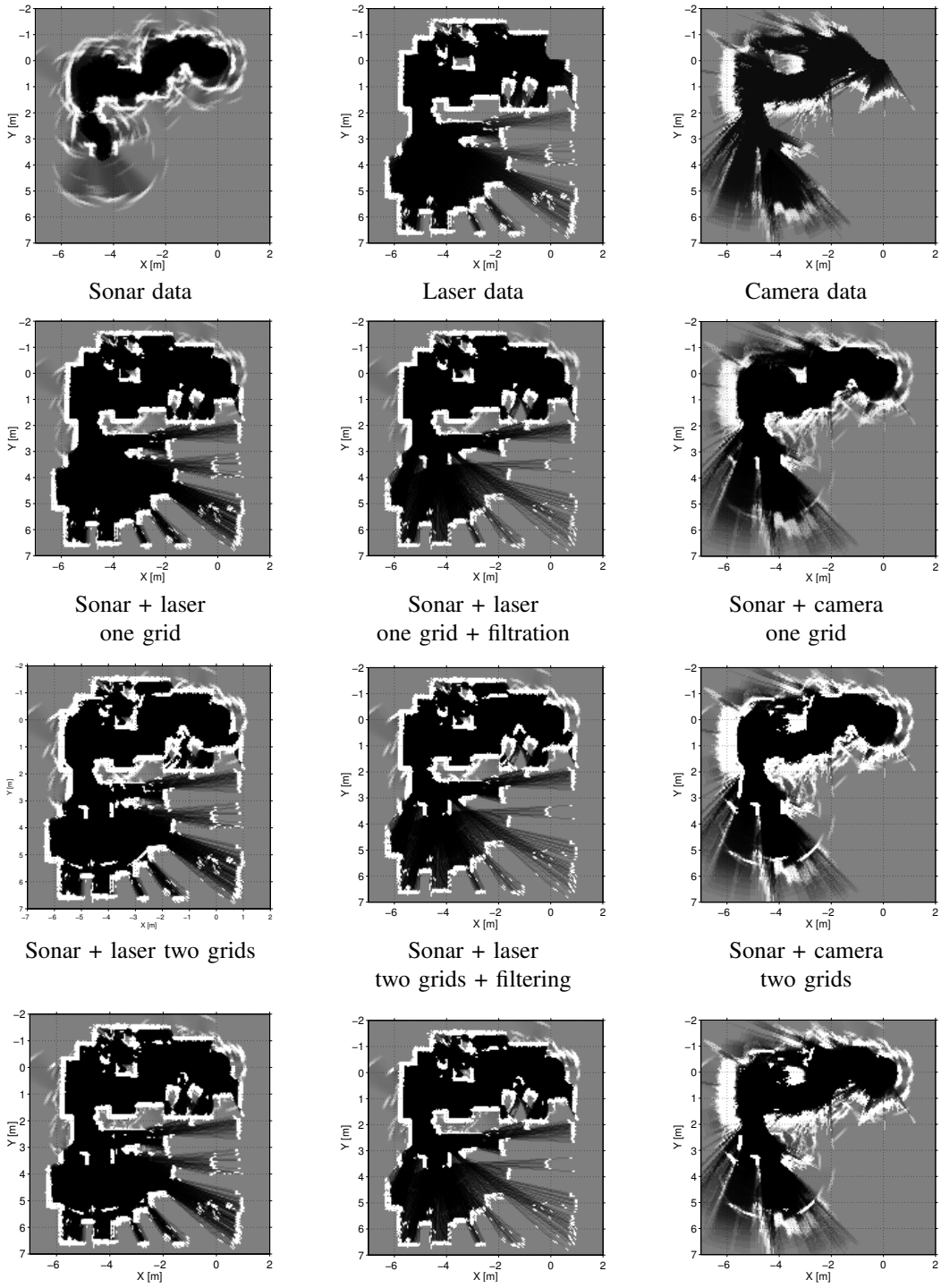

Fig. 12. Comparison of the occupancy grid from monocular camera, sonar and laser rangefinders and their mutual data fusion with different approaches.

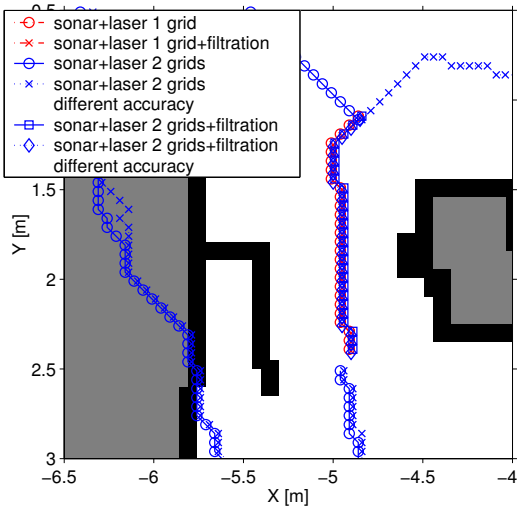

(a) Case I

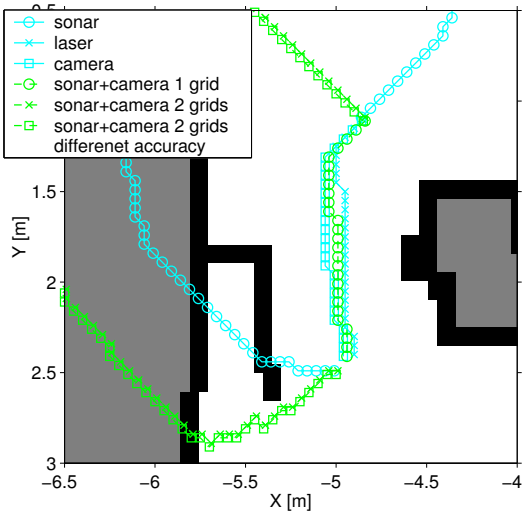

(b) Case II

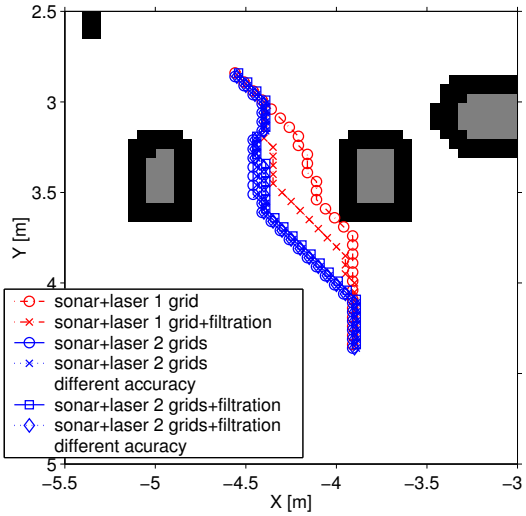

(c) Case III

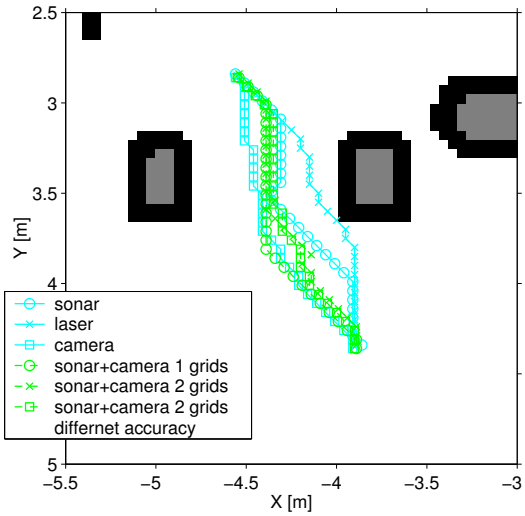

(d) Case IV

Fig. 13. Path planning results in different situations with pattern grid